HOSTED BY

ELSEVIER

Available online at www.sciencedirect.com

ScienceDirect

Soils and Foundations 59 (2019) 1182–1192

www.elsevier.com/locate/sandf

Technical Paper

Investigation of long-term behaviour of thermal wall by finite element analysis

Mei Yin [a], Yi Rui [b,*]

[a] Department of Civil and Environmental Engineering, Brunel University, UK
[b] Centre for Smart Infrastructure & Construction, Department of Engineering, University of Cambridge, UK

Received 5 November 2018; received in revised form 14 February 2019; accepted 28 March 2019
Available online 28 September 2019

Abstract

Energy foundations utilise the natural thermal energy stored underground for the space heating and/or cooling of buildings. This technology can be used for lowering carbon dioxide gas emissions. However, there has been very limited research on the effects of cyclic heating and cooling on the structural performance of thermo-active diaphragm walls (thermal walls). An investigation of the long-term behaviour of a thermal wall is conducted in this study by a finite element analysis. The complex thermo-hydro-mechanical (THM) responses due to the operation of the thermal wall are analysed. With no operation of the thermal wall, the earth pressure and the wall movement change due to the dissipation of the excess pore pressure developing from the construction. However, there is only a small change in the bending moment of the wall. With the operation of the thermal wall, the thermal differential across the diaphragm wall induces thermal strain, and therefore, an increase in curvatures, resulting in an increase in the bending moment compared with no operation of the thermal wall. This study shows the necessity of examining the thermally induced effects of a thermal wall in the design, including variations in the bending moment of the wall, the cyclic changes in the earth pressure acting on the diaphragm wall, and the thermally induced soil shrinkage/expansion.

Keywords: Thermal wall; Finite element; Bending moment; Thermo-hydro-mechanical coupling

1. Introduction

Two major challenges faced by modern society are securing energy and lowering carbon dioxide gas emissions. Ground Source Heat Pump (GSHP) technology has the great potential to aid in the remediation of these problems, since it is a sustainable energy-providing technology that uses soil as a heat exchange medium. Recent advances incorporate the ground heat exchanger (GHE) into various ground-embedded structures, such as tunnels, piles, and diaphragm walls (Brandl, 2006; Adam and Markiewicz, 2009; Amis and Nicholson et al., 2013). The number of GHEs being installed in foundation piles, also known as thermal piles, is growing rapidly in the world. (e.g., Bourne-Webb et al., 2009; Bourne-Webb, 2013; Laloui and Donna, 2011; Rui and Soga, 2018). However, compared to thermal piles, knowledge of the performance of thermal walls, in which heat exchangers are embedded, is rather limited. Most of the previous studies on thermo-active diaphragm walls (thermal walls) only focused on the temperature performance, in terms of the heating/cooling capacity (Brandl, 2006; Adam and Markiewicz, 2009), the thermal conductivity of the ground (Amis et al., 2010; Amis, 2011), and the heat transfer performance of the heat exchangers (Xia et al., 2012). However, when designing thermal walls, one principle is that the negative impact of thermal loads on the ability of the diaphragm wall to sup-

Peer review under responsibility of The Japanese Geotechnical Society.
* Corresponding author at: Department of Engineering, Trumpington Street, Cambridge CB2 1PZ, UK.
E-mail address: YR228@cam.ac.uk (Y. Rui).

https://doi.org/10.1016/j.sandf.2019.03.017

port the mechanical load of the building must be controlled. Hence, investigating the mechanical behaviour of thermal walls is another crucial task. Stewart et al. (2014) evaluated the thermal effect on the deformation behaviour of a retaining wall. They found that the thermal deformations of the diaphragm wall were reduced due to the confining effects of the unsaturated backfill. Sterpi et al. (2017) performed a coupled thermo-mechanical analysis of a thermal wall using the finite element method. Their results showed that changes in the axial force and bending moment induced by the variations in temperature are significant. On the other hand, a similar finite element analysis, performed by Bourne-Webb et al. (2016), showed that heat exchanges have little effect on the mechanical behaviour of the diaphragm wall because of the relatively uniform distribution of temperature across the diaphragm wall. Rui and Yin (2017) investigated the wall–soil interaction behaviour under both thermal and mechanical loading. It was found that the thermally induced bending moment of the diaphragm wall is mainly caused by the thermal differential across the wall.

In this paper, following the work of Rui and Yin (2017), a series of FE analyses on a thermal wall was conducted. The main purpose was to investigate the coupled thermo-hydro-mechanical performance of a thermal wall installed in London, involving the seasonal operation effects of a GSHP on the mechanical performance of the diaphragm wall. The analyses included two phases: (i) the construction phase – to calibrate the parameters of the soil model using field monitoring and (ii) the operation phase – to analyse the fully coupled THM behaviour of the soil and the diaphragm wall during heating and cooling cycles.

2. Case study

2.1. Thermal diaphragm wall in London

This research focused on a case study of a thermal wall installed at an underground station box in London. The diaphragm wall is about 1 m in thickness and 41 m in depth. The geometry of the diaphragm wall is shown in Fig. 1. The top soil of made ground and river terrace gravel has a thickness of 8.4 m; it is underlain by London Clay with a thickness of 22.3 m and then the Lambeth Group (mixed soil layers of clay, silt, and sand) with a thickness of 21 m. Below this are Thanet Sand and Chalk, as shown in Fig. 1.

2.2. Description of thermo-hydro-mechanical (THM) coupled processes

When operating the GSHP system installed in the diaphragm wall, a complicated thermo-hydro-mechanical process occurs in the soil and the diaphragm wall, as shown in

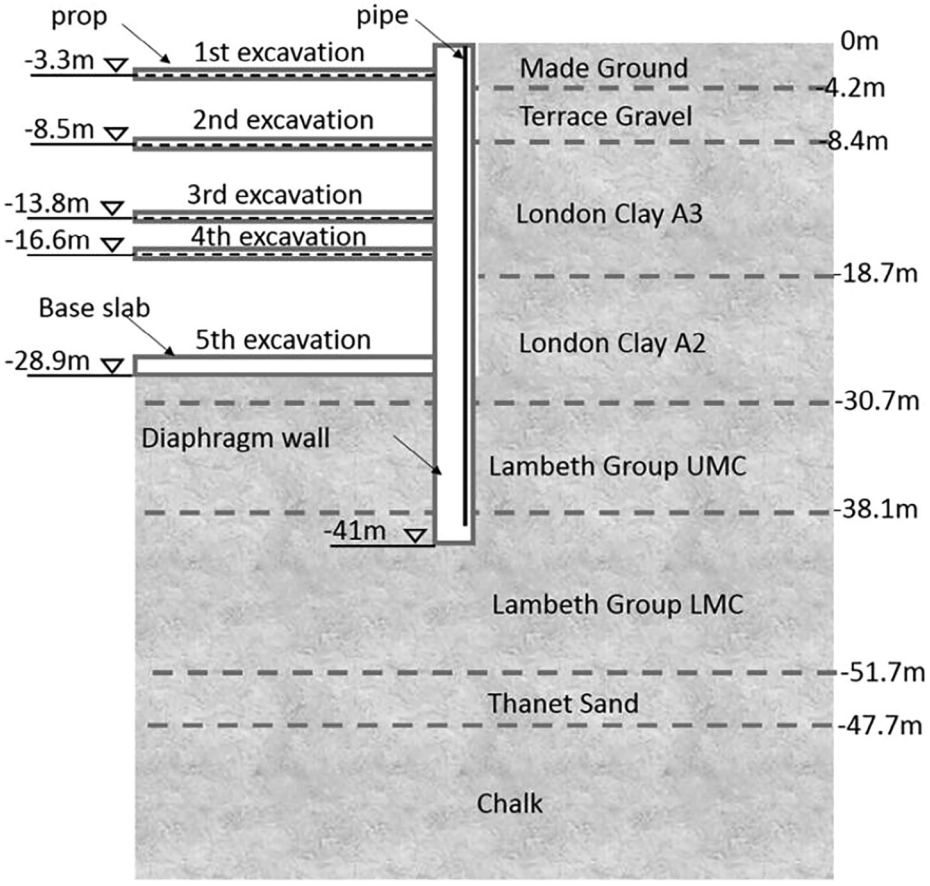

Fig. 1. Thermal wall installed in underground station box.

Fig. 2. In the subsurface, the variation in temperature causes the thermal deformation of both the pore water and the soil skeleton. Soil deformation is associated with changes in pore pressure. The transfer of pore water pressure changes the effective stress of the soil skeleton and induces heat convection. In addition, a diaphragm wall with embedded heat exchanger pipes has both thermal and mechanical contact with the surrounding soil. In this study, some assumptions have been proposed:

(1) The soil is assumed to be fully saturated.
(2) Coexisting pore fluid components and solid components are assumed to be at the same temperature.
(3) The saturated pore water flow obeys Darcy's law.
(4) The thermally induced excess pore water pressure is due to the difference in the thermal expansion coefficients between the soil skeleton and the water.

Details of the of thermo-hydro-mechanical coupled model are given in Rui and Yin (2017).

2.3. Finite element model

In order to investigate the complicated thermo-hydro-mechanical (THM) responses, the diaphragm wall was simplified into a 2-D finite element (FE) model to save computation time, as shown in Fig. 3. The absorber pipe was embedded into the diaphragm wall about 0.25 m away from the unexcavated side. The thermo-mechanical behaviour of the soils was modelled using a linear elastic model with the Mohr-Coulomb yield criterion, which is independent of the temperature. The effect of temperature on the yield surface was ignored in this case study. This is due to the heavily overconsolidated nature of London Clay and the Lambeth Group, which could be simulated as thermo-elastic materials under cyclic mechanical and thermal loading. This assumption has been validated by Rui and Soga (2018), who showed that thermally induced plastic strain is very limited during the operation of energy piles installed in London Clay. Tables 1 and 2 list all the parameters used in the finite element model.

The water table was kept constant at zero pressure at the soil surface. The pore pressure distribution was initially hydrostatic, and the left-hand-side boundary (LHS) was kept hydrostatic throughout the study. Drainage was allowed at the bottom and the LHS boundaries. The horizontal displacements were restricted at the LHS boundary. The top soil boundary was kept free, allowing for possible settlements induced by the operation of the thermal wall. The temperature boundary conditions were varied with the operation of the wall. According to the design report, the permanent conditions for the station box and the far-field soil are kept at 18 °C and 12 °C, respectively, at all times. The initial soil temperature was 12 °C, and the temperature in the pipes varied between winter and summer cycles. In this case study, a GSHP system was used to extract heat from the station (18 °C) and the surrounding soil (initially 12 °C) in winter time when the ground started

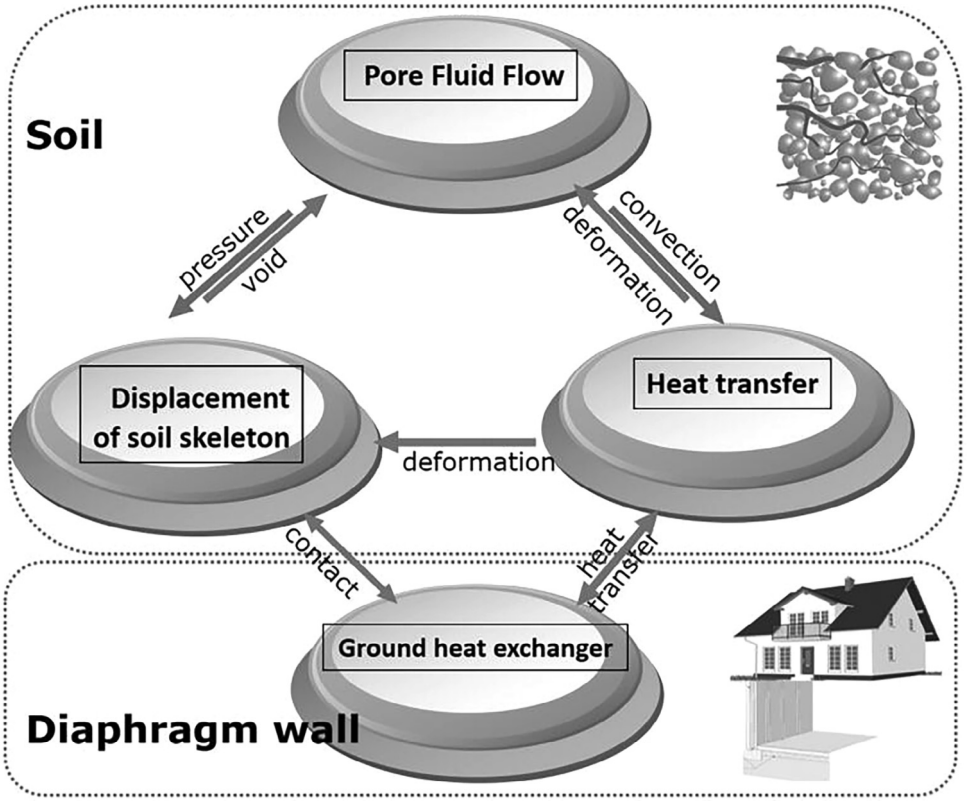

Fig. 2. Description of thermo-hydro-mechanical coupled processes.

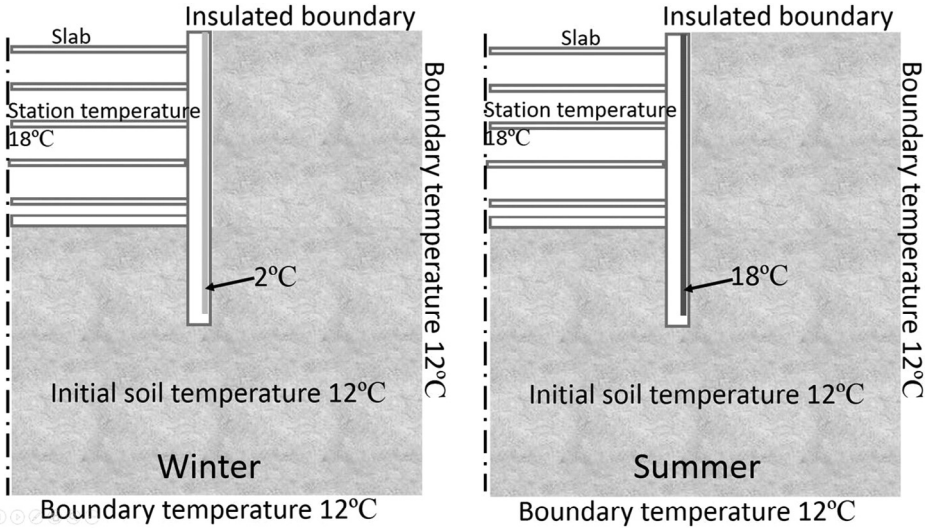

Fig. 3. Temperature boundary conditions of thermal wall: (a) winter and (b) summer.

Table 1
Mechanical properties.

Soil layer	G [kPa]	Friction angle [°]	Cohesion [kPa]	Poisson's ratio	Dilation angle [°]	Lateral pressure ratio k_0
Made Ground	4000	22.2	0	0.2	0	0.6
Terrace Gravel	20,000	35.8	0	0.2	0	0.4
London Clay A3	32,000	25	5	0.2	0	1
London Clay A2	42,000	25	5	0.2	0	1
Lambeth Group UMC	125,000	28	10	0.2	0	1
Lambeth Group LMC	112,000	23	10	0.2	0	1
Thanet Sand	167,000	27	0	0.2	0	1
Chalk	167,000	32	0	0.2	0	1

Table 2
Thermal and physical properties.

Soil layer	Thermal expansion coefficient [$\mu\varepsilon$/K]	Conductivity [W/m^2 K]	Volumetric heat capacity [kJ/m^3 K]	Permeability coefficient [m/s]	Unitweight [kN/m^3]
Made Ground	10	1.25	2800	1×10^{-4}	20
Terrace Gravel	10	1.8	2800	1×10^{-4}	21
London Clay A3	10	1.6	3200	1×10^{-10}	20
London Clay A2	10	1.6	3200	1×10^{-10}	21
Lambeth Group UMC	10	2.1	3200	1×10^{-10}	21
Lambeth Group LMC	10	2.1	3200	1×10^{-10}	21
Thanet Sand	10	1.27	2800	1×10^{-6}	21
Chalk	10	1.27	2400	1×10^{-6}	19

to cool and the temperature went down. In summer time, the GSHP system was stopped and heat was injected from the station to the ground, which caused the soil to heat up. Essentially, heat generated by the train operation is stored in the ground in summer and then extracted in winter. Hence, the temperature of the thermal pipe circuit is set at 2 °C and 18 °C for winter and summer, respectively. The applied boundary conditions for the temperature are summarised in Fig. 3.

The computation procedure for this finite element analysis (FEA) included a construction phase and an operation phase:

1. Construction Phase
   - The excavation was split into five stages; each stage involved excavating the soil to the prop level and installing the steel props.
   - The base slab was cast from the final excavation level followed by a bottom-up construction of the concrete floor slabs.
   - After the construction of the floor slabs, all the steel props were removed and the concrete slabs were constructed. At the same time, the load of a 6-storey building was applied to the base slab and the diaphragm wall.

- The modelled displacement of each stage was compared to the actual measured lateral movement data from inclinometers. The comparison was done to calibrate the stiffness values of different soils.

2. Operation Phase (20 years)
   - The cumulative effects were analysed from the construction and the heating/cooling cycles of the thermal wall.
   - Both the short- and long-term responses of the soil, with or without the operation of the thermal wall, were analysed. The comparison examined the effect of the operation of the thermal wall.

3. Results

The horizontal displacement of the diaphragm wall during the excavation is shown in Fig. 4. The wall is seen to have displaced in a curved manner, with a maximum displacement of 22 mm at a depth of 22.5 m at the end of the excavation. The maximum occurred at this point since this point lies in the area of the greatest un-propped diaphragm wall height. The displacement at depths greater than 30 m was very small since the diaphragm wall toe was embedded in the soil. The results show that the monitoring data matched well with the simulation data, especially after the final excavation. Small differences were observed when the wall was excavated to −16.6 m, which indicates that the stiffness had been a little underestimated at this state. The maximum difference was about 2 mm, but the shape of the displacement distribution was similar. In the next step (excavated to 28.9 m), the maximum difference decreased to less than 1 mm.

Fig. 5 shows the temperature contours during the operation of the thermal wall after different years of the GHSP operation. The soil temperature near the wall is seen to fall/rise during the winter/summer cycle. The effect of the changes in wall temperature on the soil is seen to decrease with the increasing distance away from the wall. The influence zone of the temperature is larger in winter than in summer because the changes in coolant temperature are greater in winter than in summer. The soil temperature below the base slab is also influenced by the changes in coolant temperature, and a distinctive thermal gradient is observed at this location. On the other hand, it is shown that the area of influence expands significantly below the base slab from the 1st year to the 10th year, which indicates that the ground needs a very long time to reach the steady state under thermal loading. The contour also shows that there is a cumulative effect of cooling (slight blue in the

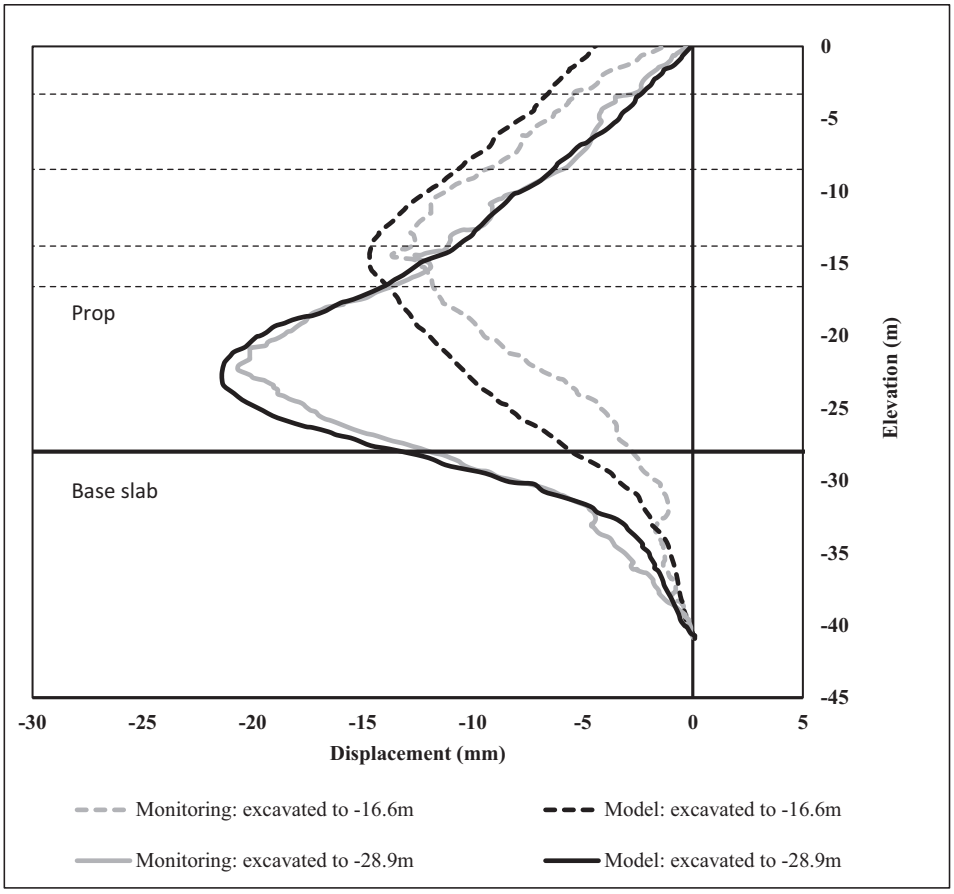

Fig. 4. Profiles of horizontal wall displacement during excavation.

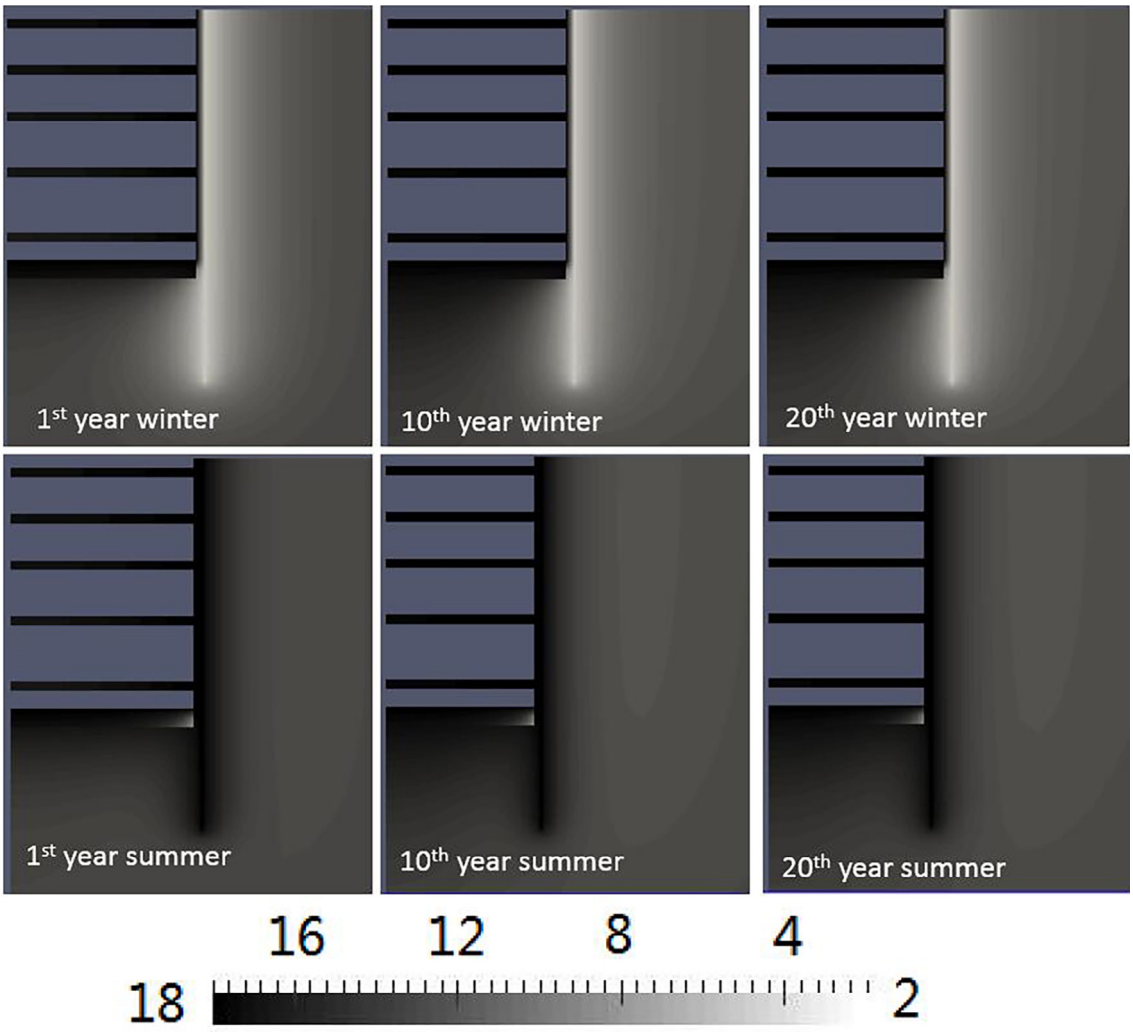

Fig. 5. Contours of temperature changes with operation of thermal wall.

soil) in the soil slightly away from the wall after 20 years of operation.

Fig. 6(a) shows the pore pressure along the wall without the operation of the thermal wall. The pore pressure is seen to slowly converge to the initial hydrostatic distribution and to find a new equilibrium during the 20 years. The results show that the negative excess pore pressure which develops in the soil adjacent to the final excavation dissipates completely within the first 10 years. On the other hand, when the GSHP is in operation, the pore pressure profile is as plotted in Fig. 6(b). Due to the thermal expansion of the water, the pore pressure in the soil adjacent to the wall increases in summer and decreases in winter. When the soil is heated, the soil skeleton and the pore fluid expand. However, due to the differences in the thermal expansion coefficient, as well as the low water permeability, negative excess pore pressure is generated in winter and positive excess pore pressure is generated in summer. The maximum difference in pore pressure between the summer and winter cycles after 20 years is about 50 kPa at the elevation of −22 m. The results also show that the changes in pore pressure between the 10th year and the 20th year are much larger than those without the operation of the thermal wall. Hence, the operation of the thermal wall delays the time needed for the excess pore pressure in the soil to dissipate.

The performance of the wall during the operation of the thermal wall is related to the changes in the soil stresses acting on the wall. When the thermal wall is not in operation, the negative excess pore pressure that developed during the wall construction dissipates over time, and the soil swells. As shown in Fig. 7(a), the total horizontal stress on the unexcavated side increases after construction over the long-term. The maximum change in horizontal stress is 150 kPa, which happens at the zone of the largest excavation. However, the changes in horizontal stress are much smaller compared to the changes in pore pressure. That is, the decrease in effective stress compensates for the increase in pore pressure. Fig. 7(b) shows the changes in the total horizontal stress along the wall on the unexcavated side with the operation of the thermal wall. When the GSHP is in operation, the lowest total horizontal stress

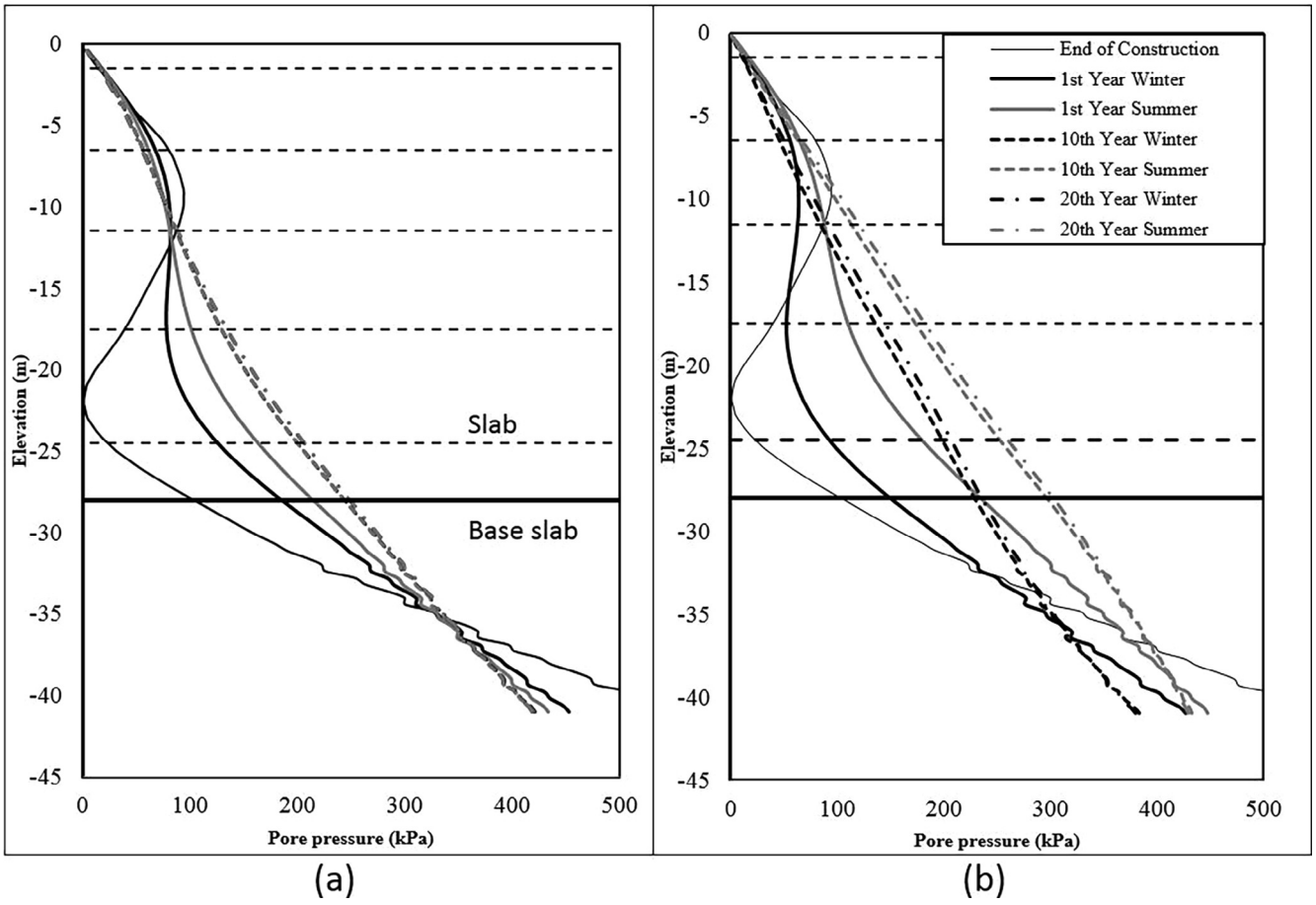

Fig. 6. Changes in pore pressure: (a) without operation of thermal wall and (b) with operation of thermal wall.

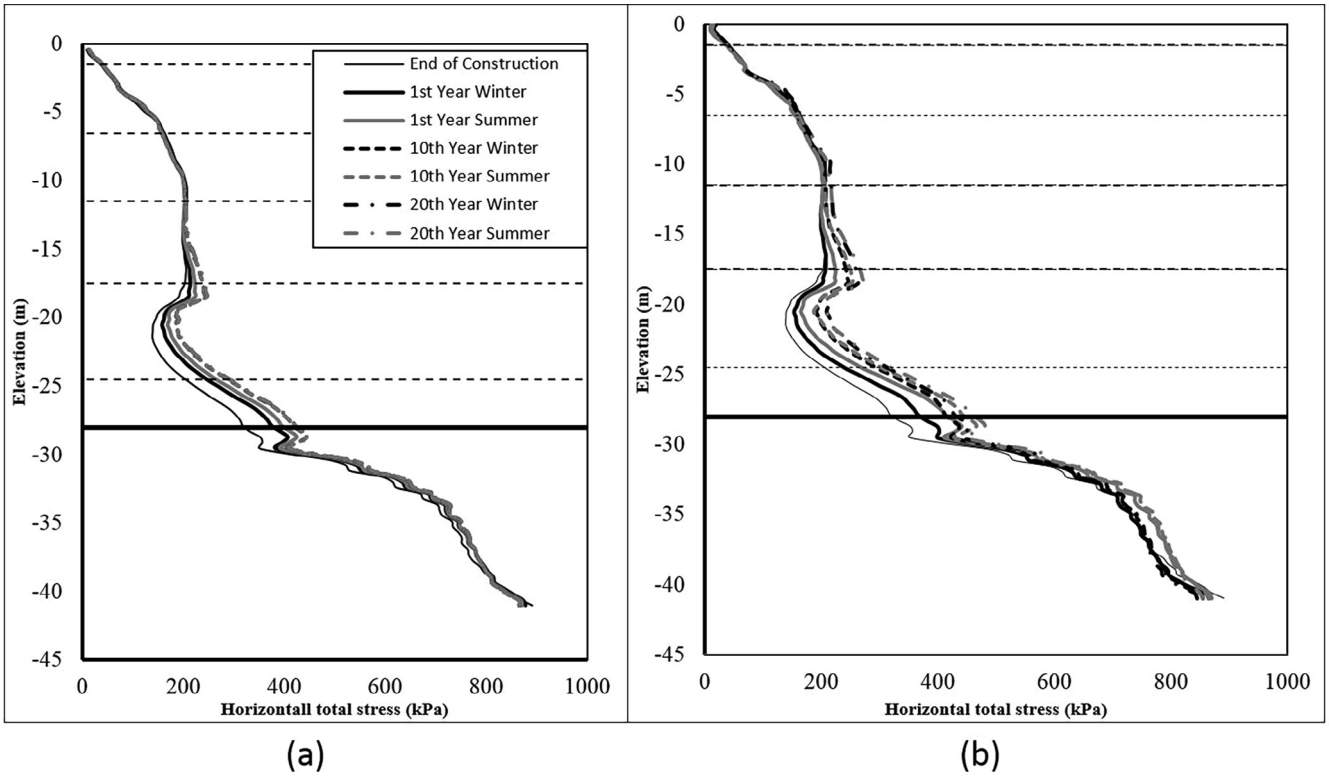

Fig. 7. Changes in total horizontal stress acting on diaphragm wall: (a) without operation of thermal wall and (b) with operation of thermal wall.

is in the first year from the excavation stage, and the stress increases over time due to swelling (a volume increase of clay due to the inflow of water). The long-term trend is similar to the stress profile obtained when the GSHP is not in operation. However, the total horizontal stress increases during the summer and decreases during the winter as the years of operation progress (Fig. 7(a)). The seasonal changes in total stress between the cycles are about 30 kPa on the unexcavated side. Two factors may influence the seasonal changes in total stress: one is the thermally induced volume changes of the soil and the pore water and the other is the thermally induced bending of the diaphragm wall. The soil and the pore water expand in summer and shrink in winter, causing the increase and decrease in total stress, corresponding to Fig. 7(b). On the other hand, the diaphragm wall bends towards the excavation side in winter, because the temperature on the unexcavated side of the wall is cold and the station (excavated) side of the wall is hot. It also causes a decrease in the total stress in winter. In summer, the bending of the wall movement pushes back toward the unexcavated side, because both sides of the diaphragm wall are hot. This would also increase the total stress in summer.

Fig. 8 shows the horizontal wall displacement relative to the end of construction. When the GSHP is not in operation, the wall shifts to the excavated side (left side) immediately after construction, with a maximum relative displacement of about −1.2 mm. Then the wall moves toward the unexcavated side (right side) over the next 20 years. The relative displacements change from −1.2 mm to −0.5 mm. As drainage under the base slab is not allowed at the excavation surface or the symmetry surface, the length of the seepage path of the soil on the excavated side is much longer than that on the unexcavated side. Hence, the consolidation on the excavated side is much slower than that on the unexcavated side. After the swelling of the soil on the unexcavated side pushes the wall to the left-hand side, consolidation under the base slab occurs gradually, leading to the wall moving back to the right side.

On the other hand, seasonal changes in relative displacement are observed when the GSHP is in operation. These changes are mainly affected by two factors: one is the thermally induced volume changes of the soil and the pore water and the other is the thermal effects on the deformation of the diaphragm wall itself. In summer, the soil on the unexcavated side expands, pushing the wall toward the excavated side. In winter, the soil on the unexcavated side shrinks, pulling the wall back toward the unexcavated side. During winter, the pipe temperature is cold and the station (excavated) side of the wall is hot, which causes variations in thermal strain in the wall, making the wall bend toward the excavated side. In summer, both sides of the wall become hot; and hence, the distribution of temperature within the diaphragm wall is uniform. It makes the wall bend back, bringing the wall back toward the unexca-

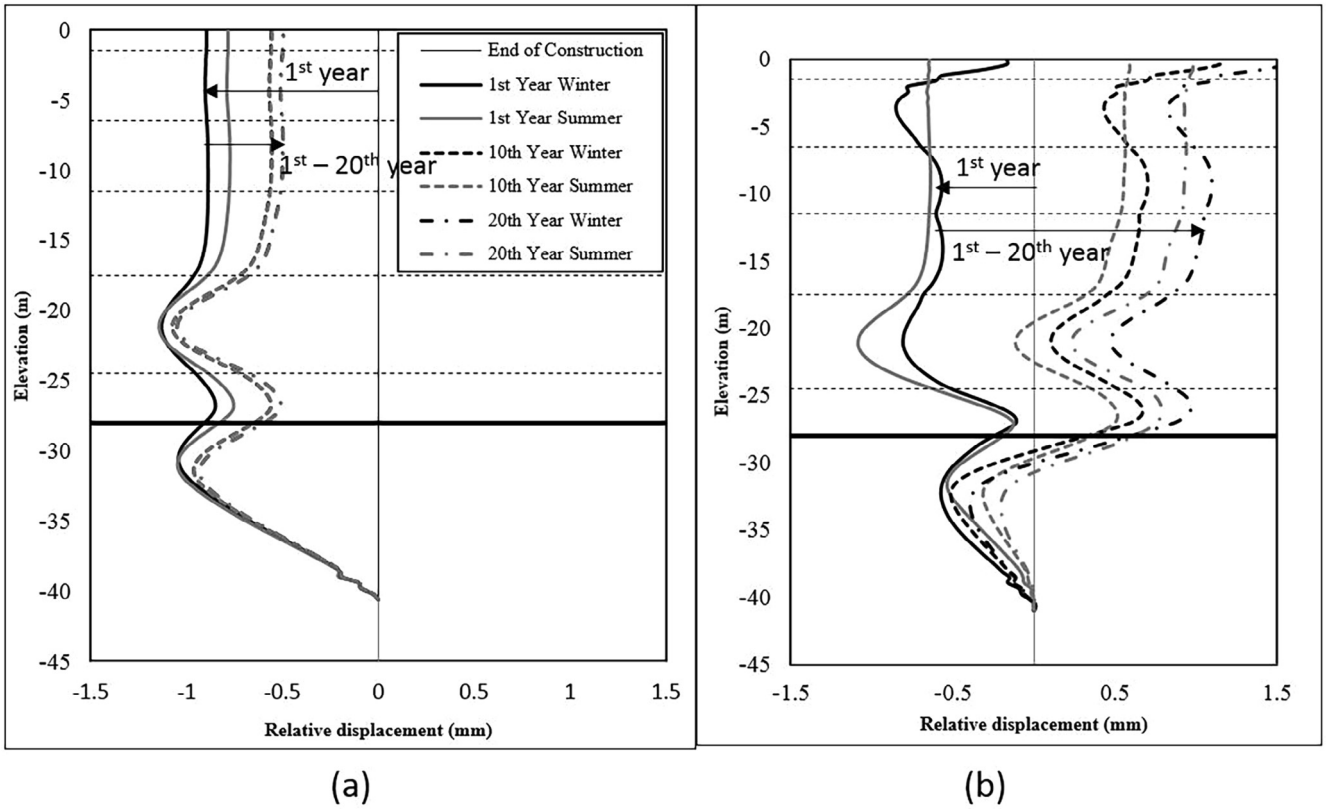

Fig. 8. Relative horizontal displacement of diaphragm wall: (a) without operation of thermal wall and (b) with operation thermal wall.

vated side. As shown in Fig. 8(b), the seasonal change in wall movement is in the same direction as the influence of the volume changes of the soil. Hence, the seasonal change in relative displacement is most dependent on the thermal effects on the volume changes of the soil and the pore water.

Fig. 9 shows the vertical displacement of the base slab. Without the operation of the thermal wall, due to the wall moving downwards during the construction stage more than the slab, there is a bulge in the base slab. Hence, if the base slab is pulled downwards due to the dissipation of excess pore pressure, as shown in Fig. 9(a), it would be squeezed in the horizontal direction, and hence, pushed to the unexcavated side at the same time. This is why there is a large horizontal displacement to the unexcavated side in the zone of the base slab during the long-term consolidation at an elevation −25 m to −28 m in Fig. 8.

Fig. 9(b) shows the vertical displacement of the base slab during the operation of the thermal wall. The slab is seen to settle by about 1.2 mm over 20 years, which is a larger settlement than that without the operation of the thermal wall. Cooling and heating makes the slab move up and down. The contours of the changes in temperature with the operation of the thermal wall, as shown in Fig. 5, show that the base slab and the soil under the base slab are always heated, and that the temperature remains constant for the whole year. Hence, the change between summer and winter is not caused by the volumetric changes due to temperature changes in the soil under the slab. Fig. 8 (b) shows that the horizontal wall moves to the left after heating and to the right after cooling above the base slab, but this change in horizontal displacement is in the opposite direction under the base slab. For this reason, the wall rotates clockwise after cooling, and rotates anticlockwise after heating. Due to the slab being fixed rigidly to the wall, it moves downward during the summer cycle and upward during the winter cycle.

Fig. 10(a) shows the wall moment without the operation of the thermal wall. After the construction, the change in moment is very small due to the limited movement of the wall during the long-term consolidation stage. There is only an increase of 100 kNm at −22 m and a decrease of 100 kNm at −32 m. This is due to the curvature of the relative horizontal displacements which increase with time in those two zones, as shown in Fig. 8(a). When the thermal wall is in operation, there is a clear difference in the bending moment between the winter and summer cycles, as shown in Fig. 10(b). An offset of 400 kNm is observed between the winter and summer cycles above the base slab level. The maximum bending moment in the wall is at −22 m and, at the base slab, where the separation between restraints (slabs) is the largest, it allows for greater bending. The soil below the base slab acts as a fixed end. The induced moment is dominated by the thermal gradient across the wall. During winter, the coolant is 10 °C below the far-field soil temperature of 12 °C, so this side of the wall shrinks. The temperature on the excavated side is always maintained at 18 °C. This temperature gradient in the wall causes expansion on the excavated side and contraction on the unexcavated side of the wall, inducing a bending moment in the wall. However, during the summer, the temperature across the wall is more uniform, so that the

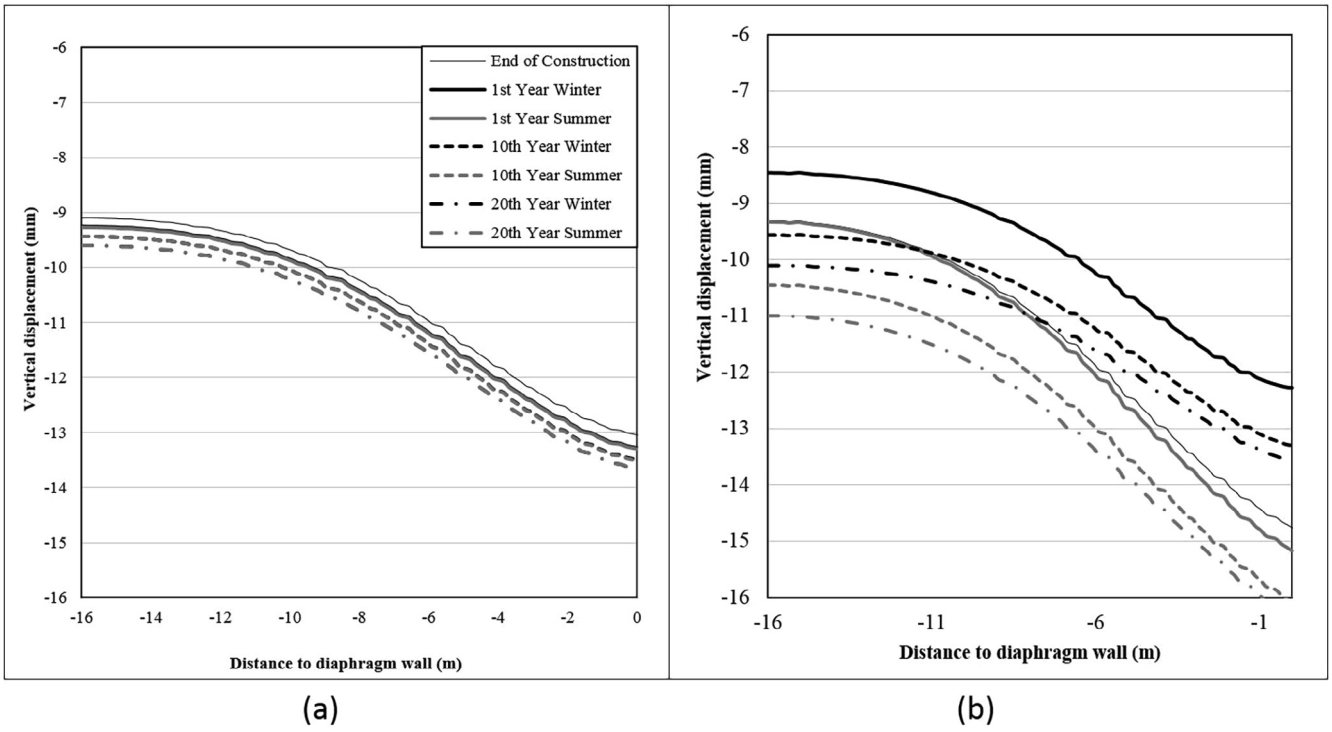

Fig. 9. Vertical displacement of base slab: (a) without operation of thermal wall and (b) with operation of thermal wall.

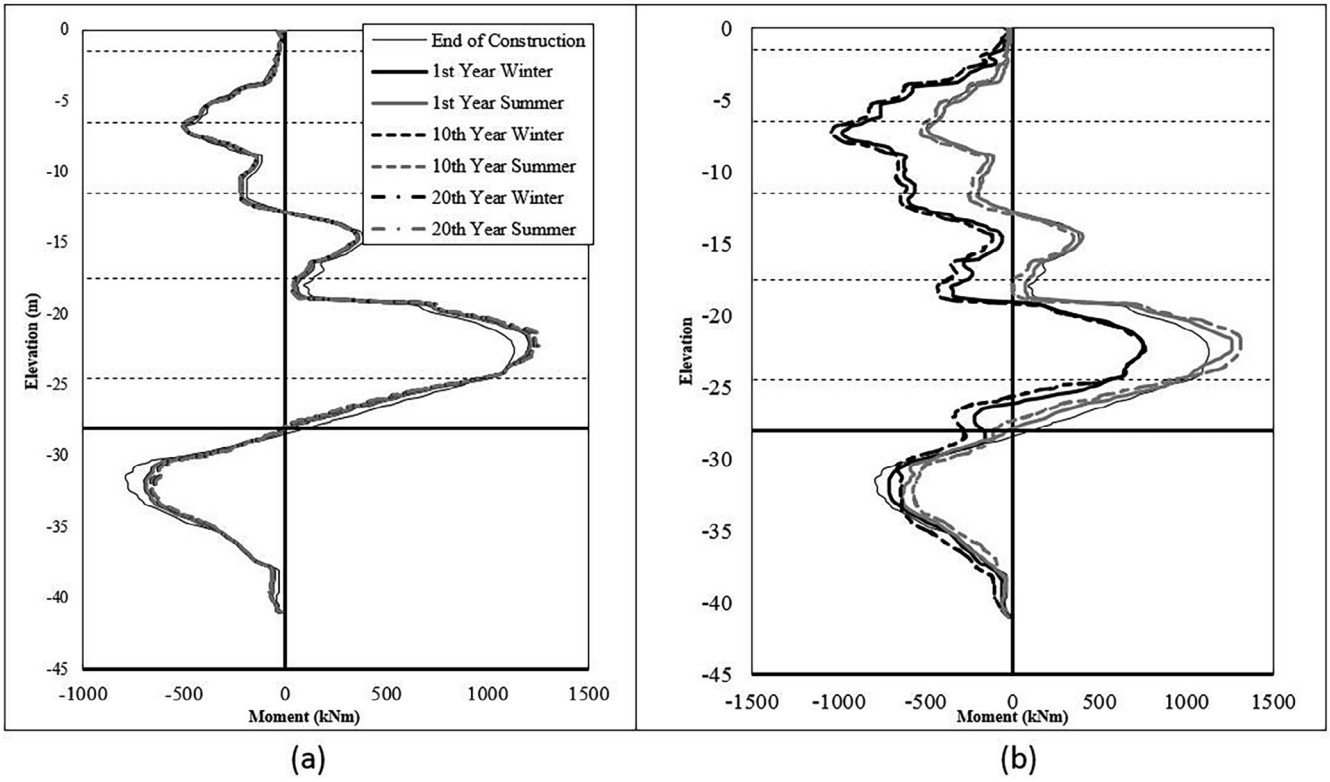

Fig. 10. Change in wall moment: (a) without operation of thermal wall and (b) with operation of thermal wall.

difference between the thermal strains is less. This results in a smaller increase in the bending moment.

The profile of the maximum bending moment in the thermal wall for different stages is shown in Fig. 11. The design moment capacity is from the project design report. All the predicted bending moment envelops are well within the design moment capacity. On the other hand, the design moment capacity is approximately three times larger than

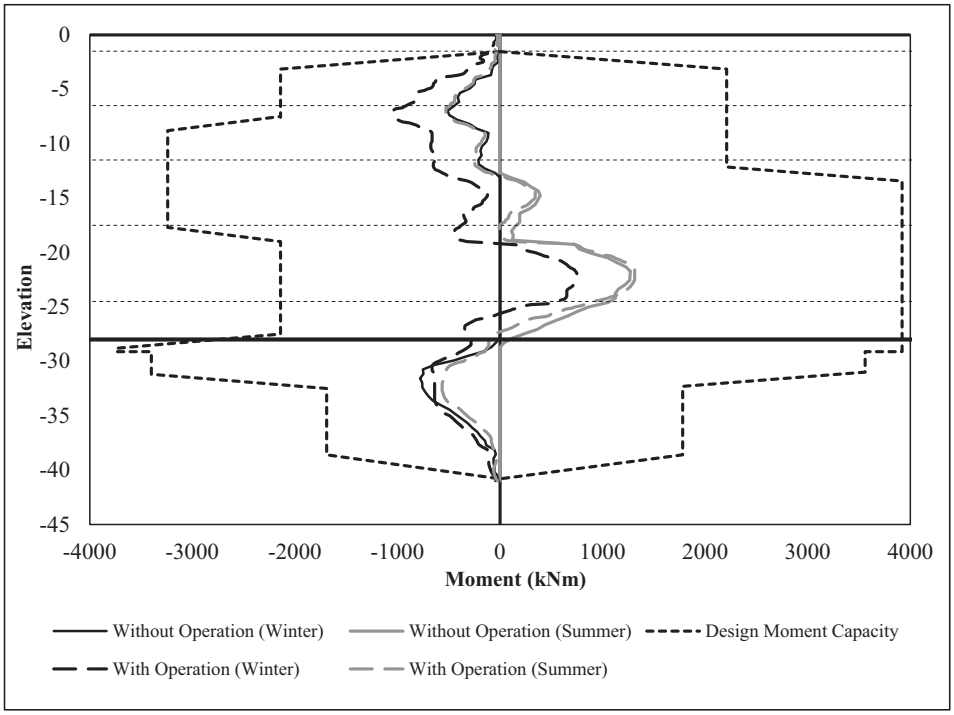

Fig. 11. Wall moment envelope at various stages of thermal wall.

the calculated bending moment envelop. This is partly due to the uncertainties of the performance of the diaphragm wall under both thermal and mechanical loading conditions, which induce a large safety factor used in the design of thermal walls. Therefore, performing a thermo-hydro-mechanical coupling analysis is quite necessary for eliminating these uncertainties, and hence, for helping to save on construction costs.

4. Conclusions

In this paper, a series of 2D FE analyses were performed on a thermal wall installed in a London underground station box using a coupled thermo-hydro-mechanical model. The following several conclusions can be made:

(1) When the thermal wall was in operation in winter, the soil surrounding the wall shrunk due to heat extraction. In summer, the ground temperature recovered and heat was stored for the following winter, but a cumulative effect of cooling was still observed over a period of 20 years, which indicates the occurrence of a thermal imbalance.
(2) The thermally induced change in the bending moment of the diaphragm wall was mainly caused by the temperature differential across the diaphragm wall. This phenomenon was seen to occur when one side of the wall was heated by the station box and the other side of the wall was cooled by the coolant in the buried pipe.
(3) With no operation of the thermal wall, the excess pore pressure induced by the excavation and construction returned to the hydrostatic state after 10 years of consolidation. With the operation of the thermal wall, this consolidation process was delayed, and the thermally induced change in pore pressure was observed to be due to the low permeability of London Clay and the Lambeth Group and the differences in the thermal expansions between the soil skeleton and the pore water.
(4) This research showed that the design of thermal walls requires examination of the thermally induced effects, including cyclic variations in the bending moment, changes in the earth pressure acting on the wall, and infrastructure settlement due to long-term changes in the ground temperature and the pore pressure.

References

Adam, D., Markiewicz, R., 2009. Energy from earth-coupled structures, foundations, tunnels and sewers. Geotechnique 59 (3), 229–236.
Amis, T., Robinson, C., Wong, S., 2010. Integrating geothermal loops into the diaphragm walls of the Knightsbridge Palace Hotel project. EMAP-Basements Underground Struct.
Amis, T., 2011. Energy Foundations in the UK [online]. Available from: <http://www.gshp.org.uk/GroundSourceLive2011/TonyAmis_Piles_gsl.pdf>.
Bourne-Webb, P.J., Amatya, B., Soga, K., Amis, T., Davidson, C., Payne, P., 2009. Energy pile test at Lambeth College, London: geotechnical and thermodynamic aspects of pile response to heat cycles. Géotechnique 59 (3), 237–248.
Bourne-Webb, P., 2013. Observed response of energy geostructures. In: Laloui, L., Di Donna, A. (Eds.), Energy Geostructures: Innovation in Underground Engineering, pp. 45–77.
Bourne-Webb, P.J., Freitas, T.B., da Costa Gonçalves, R.A., 2016. Thermal and mechanical aspects of the response of embedded retaining walls used as shallow geothermal heat exchangers. Energy Build. 125, 130–141.
Brandl, H., 2006. Energy foundations and other thermo-active ground structures. Geotechnique 56 (2), 81–122.
Laloui, L., Di Donna, A., 2011. Understanding the behaviour of energy geo-structures. Proceedings of the Institution of Civil Engineers-Civil Engineering. Thomas Telford Ltd, pp. 184–191.
Nicholson, D.P., Chen, Q., Pillai, A., Chendorain, M., 2013. Developments in thermal pile and thermal tunnel linings for city scale GSHP systems. Proceedings of the 38th Workshop on Geothermal Reservoir Engineering.
Rui, Y., Yin, M., 2017. Thermo-hydro-mechanical coupling analysis of a thermo-active diaphragm wall. Can. Geotech. J. 55 (5), 720–735.
Rui, Y., Soga, K., 2018. Thermo-hydro-mechanical coupling analysis of a thermal pile. Proceedings of the Institution of Civil Engineers-Geotechnical Engineering, pp. 1–19.
Sterpi, D., Coletto, A., Mauri, L., 2017. Investigation on the behaviour of a thermo-active diaphragm wall by thermo-mechanical analyses. Geomech. Energy Environ. 9, 1–20.
Stewart, M.A., Coccia, C.J.R., McCartney, J.S., 2014. Issues in the implementation of sustainable heat exchange technologies in reinforced, unsaturated soil structures. GeoCongress. ASCE, Reston, VA, pp. 4066–4075.
Xia, C., Sun, M., Zhang, G., Xiao, S., Zou, Y., 2012. Experimental study on geothermal heat exchangers buried in diaphragm walls. Energy Build. 52, 50–55.